

## Pseudo Catalytic Ammonia Synthesis by Lithium-Tin Alloy

Toshiro Yamaguchi<sup>b</sup>, Keita Shinzato<sup>c</sup>, Kyohei Yamamoto<sup>d</sup>, Yongming Wang<sup>e</sup>, Yuki Nakagawa<sup>d</sup>, Shigehito Isobe<sup>d</sup>, Tomoyuki Ichikawa<sup>f</sup>, Hiroki Miyaoka<sup>a\*</sup>, Takayuki Ichikawa<sup>a,b,c</sup>

<sup>a</sup>Natural Science Center for Basic Research and Development, Hiroshima University 1-3-1, Kagamiyama, Higashi-Hiroshima, 739-8530, Japan

<sup>b</sup>Graduate School of Integrated Arts and Sciences, Hiroshima University, 1-7-1 Kagamiyama, Higashi-Hiroshima 739-8521, Japan

<sup>c</sup>Graduate School of Engineering, Hiroshima University 1-4-1, Kagamiyama, Higashi-Hiroshima, 739-8527, Japan

<sup>d</sup>Graduate School of Engineering, Hokkaido University, N-13, W-8, Sapporo 060-8278, Japan

<sup>e</sup>Creative Research Institution, Hokkaido University, N-21, W-10, Sapporo 001-0021, Japan

<sup>f</sup>Hydrolabo Inc. 3-10-31, Kagamiyama, Higashi-Hiroshima, 739-0046, Japan

### Abstract

In this work, nitrogenation, ammonia generation, regeneration reactions of lithium-tin alloy is investigated as pseudo catalytic process of ammonia synthesis.  $\text{Li}_{17}\text{Sn}_4$  synthesized by thermochemical method at 500 °C can react with 0.1 MPa of  $\text{N}_2$  below 400 °C. Nano or amorphous lithium nitride would be formed by the nitrogenation. By reaction of the nitrogenated samples and  $\text{H}_2$ , ammonia is generated at 300 °C under 0.1 MPa. The initial alloy phase  $\text{Li}_{17}\text{Sn}_4$  is regenerated below 350 °C from the products after the ammonia generation process. Based on the above three step process, ammonia can be pseudo-catalytically synthesized from  $\text{N}_2$  and  $\text{H}_2$  below 400 °C under ambient pressure. Furthermore, the reactivity for the ammonia synthesis using Li-Sn alloy is preserved during the  $\text{NH}_3$  synthesis cycles due to the characteristic reaction process based on the Li extraction and insertion.

Keywords: Ammonia, Lithium alloy, Catalytic Process, Nitrogen, Hydrogen

\*Corresponding author.

Hiroki Miyaoka, e-mail: [miyaoka@h2.hiroshima-u.ac.jp](mailto:miyaoka@h2.hiroshima-u.ac.jp), TEL&FAX: +81-82-424-4604

## Introduction

So far, ammonia ( $\text{NH}_3$ ) is mainly synthesized as a material of chemical fertilizer by Haber–Bosch process, which is well known as a mass production technique of  $\text{NH}_3$ . To effectively produce massive  $\text{NH}_3$ , high temperature and pressure process is used from thermodynamic and kinetic reasons. In addition, catalysts are required to dissociate nitrogen ( $\text{N}_2$ ) and hydrogen ( $\text{H}_2$ ) molecules, and currently the iron based catalyst is utilized because of low cost and suitable activity. On the other hand, research on the catalysts for the  $\text{NH}_3$  synthesis process are continued<sup>1-5</sup>. In recent years,  $\text{NH}_3$  is recognized as an attractive energy storage and transportation medium for effective utilization of fluctuated natural energy because of the high gravimetric and volumetric energy density<sup>6</sup>. In this situation, the small-scale and distribution-type systems of  $\text{NH}_3$  synthesis are required because of unsuitability for downsizing the Haber–Bosch process. Therefore, the  $\text{NH}_3$  synthesis process should be operated at lower temperature and pressure than those of conventional ones.

With increase in the above interests for  $\text{NH}_3$  recently, various types of catalysts are proposed to synthesize  $\text{NH}_3$  with highly activity or under mild conditions, Ruthenium (Ru)-based catalysts<sup>7, 8</sup>, Ru loaded electrides<sup>9-11</sup>, Ru-Cs catalyst with electric field<sup>12</sup>, complexes<sup>13-18</sup>, oxihydride<sup>19</sup>, molten-sodium<sup>20</sup>, transition-metal composite<sup>21</sup>, other compounds such as carbide and nitride<sup>22-28</sup>, and systems including electrochemical process<sup>29, 30</sup>.

In addition, the  $\text{NH}_3$  synthesis processes based on chemical reaction using lithium nitride ( $\text{Li}_3\text{N}$ ) are also reported<sup>31, 32</sup>. Although  $\text{NH}_3$  can be produced under milder conditions than conventional catalytic processes by using atomic state of N in  $\text{Li}_3\text{N}$  as N-source, regeneration of  $\text{Li}_3\text{N}$  from the stable by-products is difficult. If Li can be generated by reducing the products,  $\text{Li}_3\text{N}$  is easily formed by the reaction with  $\text{N}_2$  because metallic state Li possesses high dissociation properties of  $\text{N}_2$  molecule even at room temperature<sup>32</sup>. However, the Li generation from stable materials such as LiH and LiOH is thermodynamically difficult, and then more than 500 °C is necessary for the reduction. As a result, the above  $\text{NH}_3$  synthesis systems consume materials or require complicated multi-step reactions by using high temperature and/or electrochemical processes for the  $\text{Li}_3\text{N}$  regeneration. It is

reported that Li alloys ( $\text{Li}_x\text{M}$ :  $\text{M}=\text{C}, \text{Si}, \text{Ge}, \text{Sn}$ ) reversibly absorb and desorb  $\text{N}_2$  below  $550\text{ }^\circ\text{C}$  by following reaction<sup>33</sup>,



The alloys are nitrogenated below  $450\text{ }^\circ\text{C}$  to form low-composition Li alloys, and especially the nitrogenation of  $\text{Li}_{22}\text{Sn}_5$  alloy proceed from around room temperature. The results suggest that Li in the alloys shows similar  $\text{N}_2$  dissociation properties to the metallic Li. The  $\text{Li}_3\text{N}$  and M mixture prepared as ideal products react in wide temperature range  $100\text{-}550\text{ }^\circ\text{C}$  to form Li alloys with  $\text{N}_2$  desorption. The reaction temperature of the alloy formation is lower than the regeneration temperature of Li from  $\text{Li}_3\text{N}$ , which is higher than  $600\text{ }^\circ\text{C}$ . The reversible nitrogenation/denitrogenation of the Li alloy is based on the high  $\text{N}_2$  dissociation properties and diffusivity of Li. The similar reversible reactions are found in the case of  $\text{H}_2$  as follows,



The hydrogenation and dehydrogenation of all the systems can be operated below  $500\text{ }^\circ\text{C}$  by destabilizing LiH by the reaction with  $\text{M}^{34}$ .

In this work, the pseudo catalytic process of  $\text{NH}_3$  synthesis by using Li-Sn alloy is proposed, in which it is composed of the nitrogenation,  $\text{NH}_3$  generation by reaction of the nitrogenated alloy with  $\text{H}_2$ , and regeneration (reformation of initial alloy). The reaction properties of the Li-Sn alloy for each process are investigated by gas-switching experiments, and moreover the  $\text{NH}_3$  generation properties via reaction between Li alloy and  $\text{H}_2\text{-N}_2$  mixed gas.

## Experiments

Lithium (Li,  $99\geq\%$ ) and tin (Sn,  $99.99\%$ ) were purchased from Sigma Aldrich and Kojundo Chemical Lab. as starting materials, respectively. To synthesize  $\text{Li}_{17}\text{Sn}_4$ , Li and Sn were weighed and mixed with a molar ratio of 17:4 (4.25:1). Then, the mixture was heat-treated at  $500\text{ }^\circ\text{C}$  for 12 h with  $5\text{ }^\circ\text{C}/\text{min}$  of heating rate under  $0.1\text{ MPa}$  of Ar.

The following thermal reaction properties were investigated by thermogravimetry (TG) (Rigaku, TG8120),

which was placed into a grove box (Miwa MFG) filled with purified Ar (>99.9999%), and the generated gases were *in-situ* analyzed by mass spectroscopy (MS) (Canon Anelva Corporation, M-QA200TS). The nitrogenation of the Li-Sn alloy was performed under 0.1 MPa of N<sub>2</sub> with flow rate of 300 cm<sup>3</sup>/min at temperature range from room temperature to 500 °C with a heating rate of 5 °C/min. The nitrogenated Li-Sn alloy was heated up to 300 °C with heating rate of 5 °C/min under 0.1 MPa of H<sub>2</sub> with flow rate of 300 cm<sup>3</sup>/min to investigate the NH<sub>3</sub> generation properties. The heat treatment of products obtained by the above reactions with N<sub>2</sub> and H<sub>2</sub> was carried out under 0.1 MPa of Ar (inert gas) with flow rate of 300 cm<sup>3</sup>/min up to 500 °C with a heating rate of 5 °C/min. The above 3-steps processes were repeated 3 times to examine cyclic properties. In addition to the above gas-switching process, the conventional catalytic properties of Li alloys for the NH<sub>3</sub> synthesis process were investigated by the home-made gas flow type apparatus. The mixed gas of N<sub>2</sub> and H<sub>2</sub> with 1:3 molar ratio was used as flow gas with rate of 100 cm<sup>3</sup>/min (H<sub>2</sub>: 75 cm<sup>3</sup>/min, N<sub>2</sub>: 25 cm<sup>3</sup>/min), where the gas ratio was adjusted by mass flow controllers. The Li-Sn alloy was packed into the reactor made of SUS and heated to 500 °C by furnace. The qualitative and quantitative analyses of generated NH<sub>3</sub> was carried out by Fourier transform infra-red spectroscopy (FT-IR) with optical path length of 1.5 m (PerkinElmer, Frontier T+MCT NB). The reaction products were identified using the X-ray diffraction (XRD) measurements (Rigaku, RINT-2100, Cu K $\alpha$  radiation). In this procedure, the sample was put on a glass plate and covered by a polyimide sheet (Du Pont-Toray Co., Ltd., Kapton) in the grove box to avoid the oxidation of the sample. Transmission electron microscope (TEM) (JEOL, JEM-2010) equipped with energy dispersive spectroscopy (EDS) analyses was used to characterize the reaction products, and electron diffraction patterns were measured for the phase identification. To observe clear variation of sample by the nitrogenation, the Li-Sn alloy react with N<sub>2</sub> gas at a load lock chamber of lens barrel, and the TEM images were observed and compared before and after the nitrogenation.

## Results and Discussion

Figure 1 shows TG-MS profiles of the Li-Sn alloy under N<sub>2</sub>, H<sub>2</sub>, and Ar flow, and Figure 2 shows XRD patterns of as-synthesized Li-Sn alloy and after the above reactions, where the broken line in Fig. 1 shows temperature program for each experiment. Main diffraction peaks observed in the XRD pattern of the as-synthesized Li-Sn alloy are assigned to Li<sub>17</sub>Sn<sub>4</sub> (Li<sub>4.25</sub>Sn) phase. To investigate the

reaction between  $\text{Li}_{17}\text{Sn}_4$  and  $\text{N}_2$ , the sample was heated up to 500 °C under 0.1 MPa  $\text{N}_2$  flow as shown in Figure 1(a). Here, although the reactivity of Li-Sn alloy with  $\text{N}_2$  gas around room temperature was examined, no weight change was observed.

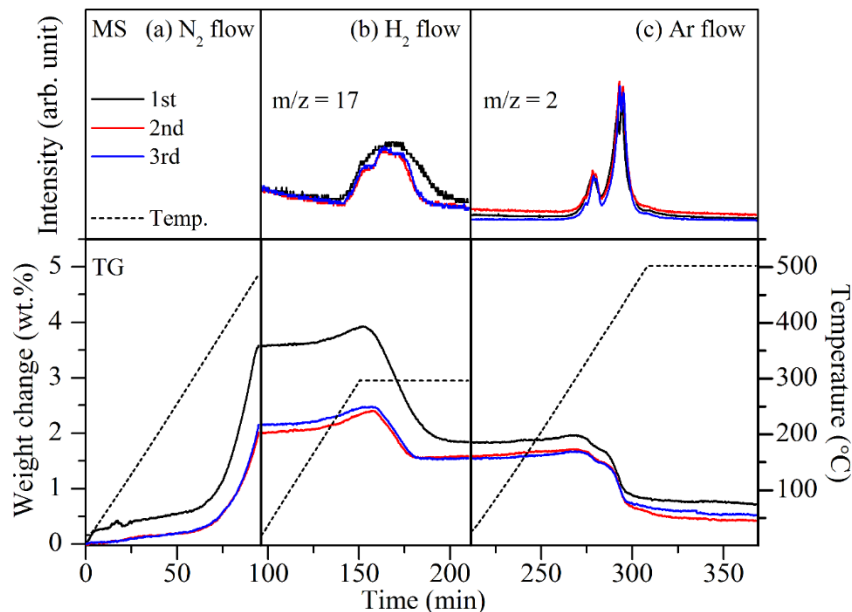


Figure 1 TG-MS profiles of  $\text{Li}_{17}\text{Sn}_4$  under 0.1 MPa of (a) $\text{N}_2$ , (b) $\text{H}_2$ , and (c)Ar flow conditions.

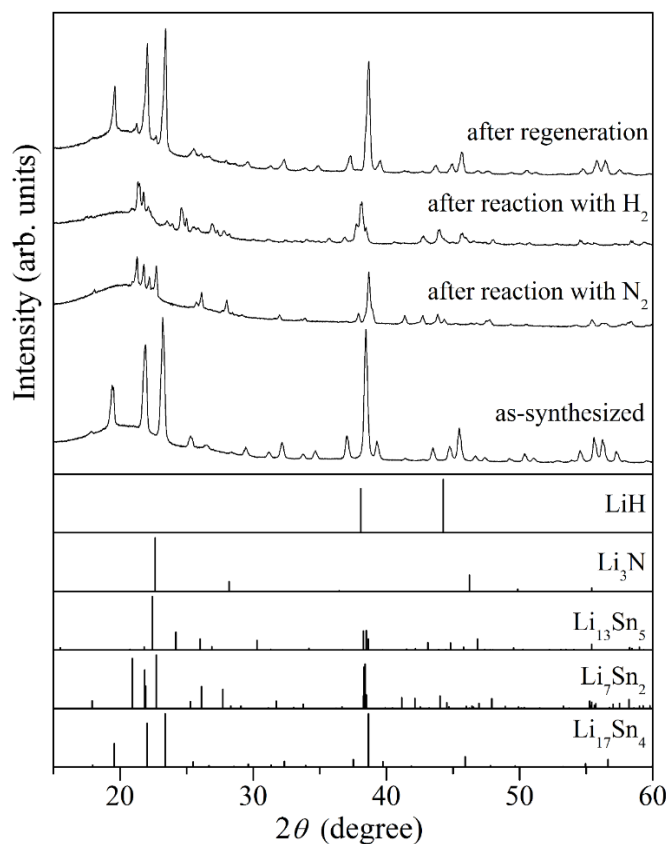


Figure 2 XRD patterns of the as-synthesized  $\text{Li}_{17}\text{Sn}_4$  alloy and the products after the reactions.

The weight of the sample began to gradually increase when the heating program started, indicating that exothermic nitrogenation gradually proceeded around 50 °C. The reaction kinetics of nitrogenation is significantly changed around 400 °C due to the thermal activation. The XRD pattern of the sample after the reaction with N<sub>2</sub> corresponded to mainly Li<sub>7</sub>Sn<sub>2</sub> (Li<sub>3.50</sub>Sn) phase, and some small peaks were assigned to Li<sub>13</sub>Sn<sub>5</sub> (Li<sub>2.60</sub>Sn) phases. By the reaction with N<sub>2</sub>, Li<sub>17</sub>Sn<sub>4</sub> was converted into the alloys with lower Li concentration than starting alloy as follows,



It is expected that the nano-sized or amorphous Li<sub>3</sub>N is formed as the reaction product because no other products are found in the XRD patterns. The weight gain estimated from the above equation is 2.4 wt.%. However, the value obtained from experiment was about 3.5 wt.%. The yield in excess of 100% would be caused by the coexistence of the lower Li composition phases such as Li<sub>13</sub>Sn<sub>5</sub> than Li<sub>7</sub>Sn<sub>2</sub> in the reaction product. In fact, it is reported that Li<sub>22</sub>Sn<sub>5</sub> was converted into Li<sub>13</sub>Sn<sub>5</sub> under 0.1 MPa N<sub>2</sub> pressure<sup>33</sup>. To characterize the reaction process of the nitrogenation, quasi *in-situ* TEM observation for the nitrogenation of Li<sub>17</sub>Sn<sub>4</sub> alloys was performed. TEM images, electron diffraction patterns, and results of EDS analysis are shown in Figure 3. The particle of as-synthesized Li<sub>17</sub>Sn<sub>4</sub> showed clear edge as shown in Fig. 3(a). After the reaction with N<sub>2</sub> gas, the products with low contrast were observed at surface part of Li<sub>17</sub>Sn<sub>4</sub> particle as shown in Fig. (b). In the diffraction patterns of the above particles of Fig. 3(c) and (d), Li<sub>17</sub>Sn<sub>4</sub> and Li<sub>7</sub>Sn<sub>2</sub> phases are found before and after the nitrogenation, respectively. This phase variation is consistent with the results of XRD measurements. Here, Li<sub>2</sub>O was observed as impurity phase for both results. For the other particle, the observed TEM images and its variation are similar to the above first particle as shown in Fig. 3(e) and (f).

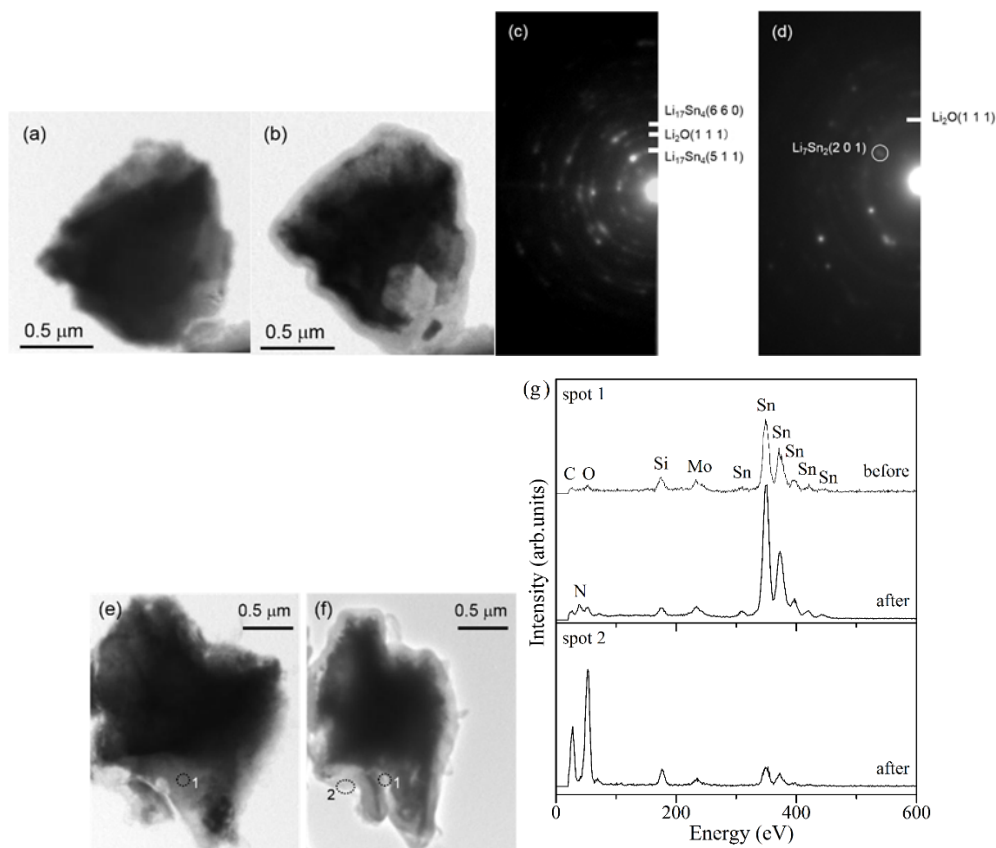


Figure. 3 TEM images of (a, e) the as-synthesized  $\text{Li}_{17}\text{Sn}_4$ , (b, f) the sample after nitrogenation, and (c, d) electron diffraction patterns, and (g) results of EDS analyses for spot 1-2 before and after the nitrogenation

The EDS analyses were carried out for spot 1 and 2 of particle shown in Fig. 3(f), and the results are shown in Fig. 3(g). No considerable amount of N atoms were observed at surface part of the products (spot 1) while the peak intensity corresponding to O atoms was higher. On the other hand, significant amount of N atoms exist at boundary area between Li-Sn alloy and products (high and low contrast parts) in EDS result of spot 2 after the nitrogenation while no peak corresponding to N was found before the reaction with  $\text{N}_2$ . The TEM image observed after the nitrogenation is similar to previous results of the *ex-situ* nitrogenated Li-Sn alloy<sup>33</sup>, indicating that the nano-sized  $\text{Li}_3\text{N}$  would be generated as products at surface part of the alloy particles. However, the generated  $\text{Li}_3\text{N}$  is very active and possibly react with tiny amount of  $\text{O}_2$ , which might be contaminated in the experiments as impurity, to form stable  $\text{Li}_2\text{O}$ . In fact,  $\text{Li}_2\text{O}$  was observed by the electron diffraction measurements. Thus, the



TEM results in this work is able to be explained by the following processes. The Li-Sn alloy reacts with N<sub>2</sub> gas, and then nano-sized/amorphous Li<sub>3</sub>N is generated as the product with low contrast near alloy surface due to Li diffusion from inside of alloy like electrode reaction of lithium ion battery. After that, the generated Li<sub>3</sub>N is changed to Li<sub>2</sub>O by the reaction with tiny O<sub>2</sub> as impurity because Li<sub>3</sub>N is quite sensitive for oxidation<sup>35</sup>. As a result, the above layered products are observed around the alloy particle.

The reaction between the nitrogenated Li-Sn alloy and H<sub>2</sub> gas was performed to synthesize NH<sub>3</sub>. If Li<sub>3</sub>N is formed during the above nitrogenation, NH<sub>3</sub> can be generated by the following equation<sup>31</sup>,



Fig. 1(b) shows TG-MS profiles of the nitrogenated alloy under 0.1 MPa of H<sub>2</sub> flow. The sample weight slightly increased from starting point of heating. The clear weight loss started from 300 °C, and then the MS signal corresponding to NH<sub>3</sub> ( $m/z = 17$ ) was observed. It is suggested that the expected NH<sub>3</sub> synthesis reaction occurred. In addition, the Li<sub>3</sub>N formation by the nitrogenation of alloy is indirectly clarified. From the XRD pattern of the products after the reaction with H<sub>2</sub> (Fig. 2), it is difficult to accurately identify the reaction products, however it is expected that the several Li-Sn phases with lower Li concentration such as Li<sub>13</sub>Sn<sub>5</sub>, Li<sub>5</sub>Sn<sub>2</sub>, Li<sub>7</sub>Sn<sub>3</sub>, and LiSn coexist. When only reaction between Li<sub>3</sub>N and H<sub>2</sub> proceeds, the Li-Sn alloy phase is not changed. The structural changes and slight increase in sample weight below 300 °C indicate the direct hydrogenation of Li-Sn alloy simultaneously occurs with the NH<sub>3</sub> generation reaction. The diffraction peaks corresponding to LiH were not found because the generated amount is small, the diffraction intensity are essentially weak, and the peak positions are overlapped with those of Li<sub>13</sub>Sn<sub>5</sub> and/or Li<sub>7</sub>Sn<sub>2</sub> phases.

Fig. 1(c) shows TG-MS profiles under Ar flow conditions of the sample after the NH<sub>3</sub> synthesis. The weight of sample began to decrease at 350 °C with H<sub>2</sub> desorption, suggesting that the reaction between Li-Sn alloys and LiH proceeded. From the XRD pattern of the products after this reaction, the main observed peaks were assigned to Li<sub>17</sub>Sn<sub>4</sub> although small peaks corresponding to the

Li-Sn alloy with other compositions were also observed. In other words, the starting phase  $\text{Li}_{17}\text{Sn}_4$  can be regenerated below 350 °C after the  $\text{NH}_3$  synthesis. As shown in the TG result, the weight change is not reached to zero (starting weight) during the 3-steps process, indicating that about 0.8 wt.% of irreversible part also exists. Thus, the reaction conditions should be optimized to enhance the reversible parts.

The TG-MS results for 2<sup>nd</sup> and 3<sup>rd</sup> cycles for the  $\text{NH}_3$  synthesis of the Li-Sn alloy are also shown in Fig. 1. For the nitrogenation, although the reactivity around room temperature is slightly lowered, the profile of the TG curve was almost similar to the 1<sup>st</sup> one. The weight gain by the reaction with  $\text{N}_2$  was about 2 wt.%. The reaction temperature of  $\text{NH}_3$  synthesis was 300 °C, which was same as that of the 1<sup>st</sup> cycle. The  $\text{NH}_3$  generation amount was also decreased due to the decrease in the amount of nitrogenation. The TG-MS profiles due to the hydrogen desorption from the sample after the  $\text{NH}_3$  synthesis for the 1<sup>st</sup> and 2<sup>nd</sup> cycles were almost consistent, where discussion of difference in the TG curves for the regeneration of alloy is essentially difficult because of low contribution of hydrogen for the sample weight. Although the synthesized amount of  $\text{NH}_3$  is relatively decreased from 2<sup>nd</sup> cycle, the reactions of nitrogenation,  $\text{NH}_3$  synthesis, and alloy regeneration become stable because results obtained in the 2<sup>nd</sup> and 3<sup>rd</sup> cycles are not clearly changed. The as-synthesized alloy has various active sites for the  $\text{NH}_3$  synthesis process, and some parts are irreversible for the reaction conditions. However, the reversible parts stably react with high durability. The high reversibility would be caused by the characteristic reaction process of this system. As described above, Li dissociates  $\text{N}_2$  and forms active nitride on the surface of alloy, indicating that the Li in alloy diffused from inside to surface parts. In the alloy regeneration process, Li located on the surface is diffused into inside and forms stable alloy phases again. Namely, it is expected that the pseudo-catalytic reactivity is preserved during the cycle because of the above reaction processes due to the Li extraction and insertion.

The Li-Sn alloy was heated up to 500 °C under mixed gas of  $\text{N}_2$  and  $\text{H}_2$  flow conditions to investigate conventional catalytic properties, which is differently from the above “pseudo catalyst” process using the gas-switching. Fig. 4 shows the IR spectra of gas passed thorough the reactor packed

with Li-Sn alloy at different temperature. From about 380 °C, the absorption peaks corresponding to stretching vibration modes of NH<sub>3</sub> were observed. The higher amount of NH<sub>3</sub> is generated in the temperature range from 400-450 °C although the amount of generated NH<sub>3</sub> is gradually decreased at higher than 450 °C. These results indicate that suitable temperature window exist for the effective NH<sub>3</sub> synthesis. The FT-IR spectrum with the highest absorption peak of NH<sub>3</sub> observed at 412 °C was quantitatively analyzed by using calibration results obtained from the analyses of reference gas with different NH<sub>3</sub> concentration, which is NH<sub>3</sub> and Ar mixed gases. As a result, the NH<sub>3</sub> concentration generated by the reaction of Li-Sn alloy was about 400 ppm, which is ten times smaller than 4320 ppm estimated from thermodynamic equilibrium state at 400 °C. Thus, the NH<sub>3</sub> synthesis properties of Li-Sn alloy as conventional catalytic processes are poor.

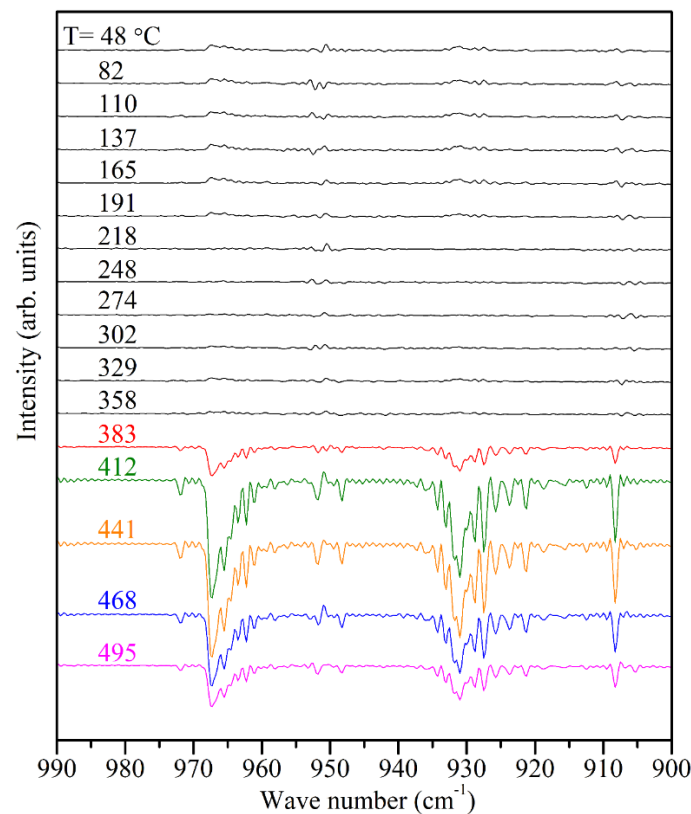


Figure 4 IR spectra of outlet gas from column with Li<sub>17</sub>Sn<sub>4</sub> alloy at different temperature

From the above experimental results, it is recognized that the Li-Sn alloy is available as “pseudo catalyst” with high durability for NH<sub>3</sub> synthesis via gas-switching processes. By using this

process,  $\text{NH}_3$  can be synthesized below 350 °C under 0.1 MPa.

## Conclusion

In this work, Li-Sn alloy ( $\text{Li}_{17}\text{Sn}_4$ ) is synthesized by thermochemical method at 500 °C. The nitrogenation properties was investigated using the TG measurements under  $\text{N}_2$  gas flow. It is found that the reaction between  $\text{Li}_{17}\text{Sn}_4$  and  $\text{N}_2$  begins at room temperature and accelerated from around 400 °C. The products obtained by the nitrogenation process is mainly  $\text{Li}_7\text{Sn}_2$  with lower Li concentration, suggesting that the Li atoms in the alloy reacts. Although  $\text{Li}_3\text{N}$  is not found in XRD patterns after the nitrogenation, it is indicated from TEM analyses that Li atoms is diffused from inside of alloy to surface part and forms nitride. The nitrogenated sample reacts with  $\text{H}_2$  to form  $\text{NH}_3$  at 300 °C under 0.1 MPa. After the  $\text{NH}_3$  generation, the product can be recycled back to initial alloy phase  $\text{Li}_{17}\text{Sn}_4$  around 350 °C. Therefore, by using the reaction of Li alloy as “pseudo catalysts”,  $\text{NH}_3$  can be synthesized below 400 °C under 0.1 MPa. Interestingly, the reactivity is not drastically changed after cycles. This phenomena would be originated in the characteristic dynamics of Li atoms during the reaction process.

## Acknowledgement

This work was supported by JSPS KAKENHI, Grant-in-Aid for Scientific Research (B), Grant Number JP17H03417. Authors are thankful to Prof. Y. Kojima for useful discussion and suggestions during the preparation of this manuscript. A part of this work was conducted at "Joint-Use Facilities: Laboratory of Nano-Micro Material Analysis" at Hokkaido University, supported by Nanotechnology Platform Program of the Ministry of Education, Culture, Sports, Science, and Technology (MEXT), Japan.

## Reference

- (1) Aika, K.; Ozaki, A. Mechanism and isotope effect in ammonia synthesis over molybdenum nitride. *J. Catal.* **1969**, *14*, 311-321.
- (2) Aika, K.; Ozaki, A. Kinetics and isotope effect of ammonia synthesis over a singly-promoted iron catalyst. *J. Catal.* **1970**, *19*, 350-352.
- (3) Aika, K.; Hori, H.; Ozaki, A. Activation of nitrogen by alkali metal promoted transition metal I. Ammonia synthesis over ruthenium promoted by alkali metal. *J. Catal.* **1972**, *27*, 424-431.
- (4) Aika, K.; Yamaguchi, J.; Ozaki, A. AMMONIA SYNTHESIS OVER RHODIUM, IRIDIUM AND PLATINUM PROMOTED BY POTASSIUM. *Chem. Lett.* **1973**, *2*, 161-164.
- (5) Aika, K. Role of alkali promoter in ammonia synthesis over ruthenium catalysts-effect on reaction mechanism. *Catal. Today* **2017**, *286*, 14-20.
- (6) Christensen, C. H.; Johannessen, T.; Sørensen, R. Z.; Nørskov, J. K. Towards an ammonia-mediated hydrogen economy? *Catalysis Today* **2006**, *111*, 140-144.
- (7) Ogura, Y.; Sato, K.; Miyahara, S.-i.; Kawano, Y.; Toriyama, T.; Yamamoto, T.; Matsumura, S.; Hosokawa, S.; Nagaoka, K. Efficient ammonia synthesis over a Ru/La<sub>0.5</sub>Ce<sub>0.5</sub>O<sub>1.75</sub> catalyst pre-reduced at high temperature. *Chemical Science* **2018**, *9*, 2230-2237.
- (8) Sato, K.; Imamura, K.; Kawano, Y.; Miyahara, S.-i.; Yamamoto, T.; Matsumura, S.; Nagaoka, K. A low-crystalline ruthenium nano-layer supported on praseodymium oxide as an active catalyst for ammonia synthesis. *Chemical Science* **2017**, *8*, 674-679.
- (9) Kitano, M.; Inoue, Y.; Yamazaki, Y.; Hayashi, F.; Kanbara, S.; Matsuishi, S.; Yokoyama, T.; Kim, S.-W.; Hara, M.; Hosono, H. Ammonia synthesis using a stable electride as an electron donor and reversible hydrogen store. *Nat Chem* **2012**, *4*, 934-940.
- (10) Kitano, M.; Kanbara, S.; Inoue, Y.; Kuganathan, N.; Sushko, P. V.; Yokoyama, T.; Hara, M.; Hosono, H. Electride support boosts nitrogen dissociation over ruthenium catalyst and shifts the bottleneck in ammonia synthesis. *Nat Commun* **2014**, *6*,
- (11) Hara, M.; Kitano, M.; Hosono, H. Ru-Loaded C12A7:e<sup>-</sup> Electride as a Catalyst for Ammonia Synthesis. *ACS Catalysis* **2017**, *7*, 2313-2324.
- (12) Murakami, K.; Manabe, R.; Nakatsubo, H.; Yabe, T.; Ogo, S.; Sekine, Y. Elucidation of the role of electric field on low temperature ammonia synthesis using isotopes. *Catal. Today* **2018**, *303*, 271-275.
- (13) Sekiguchi, Y.; Arashiba, K.; Tanaka, H.; Eizawa, A.; Nakajima, K.; Yoshizawa, K.; Nishibayashi, Y. Catalytic Reduction of Molecular Dinitrogen to Ammonia and Hydrazine Using Vanadium Complexes. *Angewandte Chemie International Edition* **2018**, *57*, 9064-9068.
- (14) Eizawa, A.; Arashiba, K.; Tanaka, H.; Kuriyama, S.; Matsuo, Y.; Nakajima, K.; Yoshizawa, K.; Nishibayashi, Y. Remarkable catalytic activity of dinitrogen-bridged dimolybdenum complexes bearing NHC-based PCP-pincer ligands toward nitrogen fixation. *Nature Communications* **2017**, *8*, 14874.
- (15) Nishibayashi, Y. Development of catalytic nitrogen fixation using transition metal-dinitrogen

complexes under mild reaction conditions. *Dalton Transactions* **2018**, 47, 11290-11297.

- (16) Shima, T.; Hu, S.; Luo, G.; Kang, X.; Luo, Y.; Hou, Z. Dinitrogen Cleavage and Hydrogenation by a Trinuclear Titanium Polyhydride Complex. *Science* **2013**, 340, 1549-1552.
- (17) Tanabe, Y.; Arashiba, K.; Nakajima, K.; Nishibayashi, Y. Catalytic Conversion of Dinitrogen into Ammonia under Ambient Reaction Conditions by Using Proton Source from Water. *Chemistry – An Asian Journal* **2017**, 12, 2544-2548.
- (18) Tanaka, H.; Arashiba, K.; Kuriyama, S.; Sasada, A.; Nakajima, K.; Yoshizawa, K.; Nishibayashi, Y. Unique behaviour of dinitrogen-bridged dimolybdenum complexes bearing pincer ligand towards catalytic formation of ammonia. *Nature Communications* **2014**, 5, 3737.
- (19) Kobayashi, Y.; Tang, Y.; Kageyama, T.; Yamashita, H.; Masuda, N.; Hosokawa, S.; Kageyama, H. Titanium-Based Hydrides as Heterogeneous Catalysts for Ammonia Synthesis. *J. Am. Chem. Soc.* **2017**, 139, 18240-18246.
- (20) Kawamura, F.; Taniguchi, T. Synthesis of ammonia using sodium melt. *Scientific Reports* **2017**, 7, 11578.
- (21) Wang, P.; Chang, F.; Gao, W.; Guo, J.; Wu, G.; He, T.; Chen, P. Breaking scaling relations to achieve low-temperature ammonia synthesis through LiH-mediated nitrogen transfer and hydrogenation. *Nature Chemistry* **2017**, 9, 64.
- (22) AlShibane, I.; Daisley, A.; Hargreaves, J. S. J.; Hector, A. L.; Laassiri, S.; Rico, J. L.; Smith, R. I. The Role of Composition for Cobalt Molybdenum Carbide in Ammonia Synthesis. *ACS Sustainable Chemistry & Engineering* **2017**, 5, 9214-9222.
- (23) Gong, Y.; Wu, J.; Kitano, M.; Wang, J.; Ye, T.-N.; Li, J.; Kobayashi, Y.; Kishida, K.; Abe, H.; Niwa, Y.; Yang, H.; Tada, T.; Hosono, H. Ternary intermetallic LaCoSi as a catalyst for N<sub>2</sub> activation. *Nature Catalysis* **2018**, 1, 178-185.
- (24) Jacobsen, C. J. H.; Dahl, S.; Clausen, B. S.; Bahn, S.; Logadottir, A.; Nørskov, J. K. Catalyst Design by Interpolation in the Periodic Table: Bimetallic Ammonia Synthesis Catalysts. *J. Am. Chem. Soc.* **2001**, 123, 8404-8405.
- (25) Laassiri, S.; Zeinalipour-Yazdi, C. D.; Catlow, C. R. A.; Hargreaves, J. S. J. The potential of manganese nitride based materials as nitrogen transfer reagents for nitrogen chemical looping. *Applied Catalysis B: Environmental* **2018**, 223, 60-66.
- (26) Laassiri, S.; Zeinalipour-Yazdi, C. D.; Catlow, C. R. A.; Hargreaves, J. S. J. Nitrogen transfer properties in tantalum nitride based materials. *Catal. Today* **2017**, 286, 147-154.
- (27) Michalsky, R.; Avram, A. M.; Peterson, B. A.; Pfromm, P. H.; Peterson, A. A. Chemical looping of metal nitride catalysts: low-pressure ammonia synthesis for energy storage. *Chemical Science* **2015**, 6, 3965-3974.
- (28) Tsuji, Y.; Ogasawara, K.; Kitano, M.; Kishida, K.; Abe, H.; Niwa, Y.; Yokoyama, T.; Hara, M.; Hosono, H. Control of nitrogen activation ability by Co-Mo bimetallic nanoparticle catalysts prepared via sodium naphthalenide-reduction. *J. Catal.* **2018**, 364, 31-39.
- (29) Amar, I.; Lan, R.; Petit, C.; Tao, S. Solid-state electrochemical synthesis of ammonia: a review.

*Journal of Solid State Electrochemistry* **2011**, *15*, 1845-1860.

- (30) Imamura, K.; Matsuyama, M.; Kubota, J. Ammonia Synthesis from Nitrogen and Water by Electricity Using an Electrochemical Cell with Ru Catalyst, Hydrogen-Permeable Pd-Ag Membrane, and Phosphate-Based Electrolyte. *ChemistrySelect* **2017**, *2*, 11100-11103.
- (31) Goshome, K.; Miyaoka, H.; Yamamoto, H.; Ichikawa, T.; Ichikawa, T.; Kojima, Y. Ammonia Synthesis via Non-Equilibrium Reaction of Lithium Nitride in Hydrogen Flow Condition. *Mater. Trans.* **2015**, *56*, 410-414.
- (32) Jain, A.; Miyaoka, H.; Kumar, S.; Ichikawa, T.; Kojima, Y. A new synthesis route of ammonia production through hydrolysis of metal – Nitrides. *Int. J. Hydrogen Energy* **2017**, *42*, 24897-24903.
- (33) Yamaguchi, S.; Ichikawa, T.; Wang, Y.; Nakagawa, Y.; Isobe, S.; Kojima, Y.; Miyaoka, H. Nitrogen Dissociation via Reaction with Lithium Alloys. *ACS Omega* **2017**, *2*, 1081-1088.
- (34) Jain, A.; Miyaoka, H.; Ichikawa, T. Destabilization of lithium hydride by the substitution of group 14 elements: A review. *Int. J. Hydrogen Energy* **2016**, *41*, 5969-5978.
- (35) Sun, Y.; Li, Y.; Sun, J.; Li, Y.; Pei, A.; Cui, Y. Stabilized Li<sub>3</sub>N for efficient battery cathode prelithiation. *Energy Storage Materials* **2017**, *6*, 119-124.